ELSEVIER

Surface Science 505 (2002) L227–L236

SURFACE SCIENCE

www.elsevier.com/locate/susc

Surface Science Letters

Surface chemistry of OH dangling bonds in vapour-deposited ice films at 128–185 K: hydrogen-bonding interactions with acetone

S. Mitlin, K.T. Leung *

Department of Chemistry, University of Waterloo, Waterloo, Ont., Canada N2L 3G1

Received 10 October 2001; accepted for publication 29 November 2001

Abstract

Sharp features corresponding to incompletely coordinated OH groups at 3700–3690 cm^{-1} have been observed in Fourier-transform infrared reflection–absorption (FTIR-RA) spectra of polycrystalline ice (pc-ice) and non-crystalline ice (nc-ice) films (obtained by vapour deposition over a wide temperature range of 128–185 K). The nature of the external surface containing the OH dangling groups remains unchanged upon film growth for the polycrystalline phase, in contrast to the nc-ice growth where the surface evolves into a convoluted openwork structure. The OH dangling bonds (db's) in an ice film provide the basic network for hydrogen bonding and other interactions for acetone adsorption. Hydrogen bonding between the adsorbates and OH db's induces ordering towards crystalline structures in the partially disordered near-surface region of pc-ice and in the structure of nc-ice films. The amounts of acetone chemisorbed on both pc-ice and nc-ice films are found to be proportional to the amounts of OH db's present in the respective ice structures. Along with the acetone–HO db complexes, FTIR-RA features attributable to van der Waals complexes and plausible intermediate clathrate–hydrate structures are found (in the spectra of pc-ice films exposed to acetone vapours). Post-deposition spectral evolution reveals the intricate surface dynamics for acetone adsorption in the hydrogen-bond-dominated system.

Keywords: Water; Polycrystalline surfaces; Infrared absorption spectroscopy; Growth; Adsorption kinetics

1. Nature of polycrystalline and non-crystalline ice films

Low-temperature micro-phases of ice continue to attract intense interest over the past decade primarily due to their important role as a common medium for organic and inorganic chemical processes at different temperature regimes in the biosphere (220–273 K) [1], atmosphere (190–220 K) [2,3], and interstellar space (10 K) [4]. The interaction of polymorph phases with the impinging molecules could lead to adsorption, clusterization and chemical modification, and diffusion in the original or modified forms into the bulk of the ice phase. The mechanisms of the interaction between the adsorbates and ice are therefore expected to depend on the bulk structure, and the surface

* Corresponding author. Tel.: +1-519-888-4567x5826; fax: +1-519-746-0435.

E-mail address: tong@uwaterloo.ca (K.T. Leung).

0039-6028/02/$ - see front matter
PII: S0039-6028(01)01914-8

properties and dynamics of specific complexes of the micro-phases that exist under different temperature and other conditions.

Despite many sometimes controversial observations, there is a general consensus among the early studies [5–9] that condensation of water vapour on a cold substrate at low pressure under the appropriate deposition conditions could lead to the formation of different non-crystalline structures below 130 K and of polycrystalline polymorphs Ic (cubic ice) and Ih (hexagonal ice) at a higher temperature. In the case of non-crystalline ice (nc-ice), the low-density amorphous ice is commonly described as a highly porous open network with nano-scale pores and therefore a significant concentration of non-compensated surface OH groups [10,11]. For the more compact high-density amorphous ice, its structure has been proposed to be similar to the low-density amorphous ice particularly in terms of the oxygen–oxygen radial distribution function but with additional water molecules occupying interstitial sites [8]. Non-crystalline structures are metastable with respect to crystalline phases Ic and Ih and consequently their formation and existence are kinetically controlled. Upon annealing to a higher temperature, nc-ice transforms irreversibly to Ic over 140–160 K [12], which in turn undergoes further irreversible phase transition to Ih over 160–240 K. The wide transition temperature range of the Ic-to-Ih transition is thought to be the result of dependence of the crystallization temperature on the size of cubic ice crystals [12]. This series of crystallization processes, which begin at temperature just above the glass-to-liquid transition, is found to be incomplete in the sense that fragments of non-crystalline micro-phases can coexist metastably with Ic over 140–210 K and with both Ic and Ih above 160 K. The nature of these non-crystalline micro-phases remains to be a subject of intense debate [8,9,12,13]. These observations suggest that the ice phase between 135 K (the onset of the glass-to-liquid transition) and 240 K (the completion of the Ic-to-Ih transformation) consists of non-crystalline and crystalline micro-phases in dynamic equilibrium, with increasing proportion of the latter phase with increasing temperature. The structural evolution of these ice micro-phases with temperature involves morphological and interfacial processes in which rearrangement of hydrogen bonds at multiple internal and external interfaces plays a key role. The reconstruction processes that accompany the phase transformations are believed to be responsible for the kinetically controlled nature of the phase transformations [12]. Clearly, the nature and composition of the ice micro-phases (the substrate) at a particular temperature have a strong effect on the types of adsorbates and their interactions with the ice structure itself. On the other hand, molecules adsorbed on the surface or trapped into the bulk of such complex could in turn affect the dynamics of the phase transformation and especially the progress of reconstruction. Indeed, very little is known about the surface complexes of the ice micro-phases over the temperature range 140–210 K.

Current understanding of the chemical properties and surface structures of nc-ice and polycrystalline ice (pc-ice) phases is based primarily on the Devlin–Buch approach, which has been developed on Fourier-transform infrared (FTIR) data of nc-ice and pc-ice nano-particles and their interactions with adsorbates of different chemical nature and complemented by molecular dynamics simulations of the surface and near-surface regions [14]. In particular, Rowland et al. observed stretching modes of three-coordinated water molecules with the H or O in the dangling bond (db) position and of relaxed four-coordinated molecules on ice nanocrystals prepared by rapid molecular expansion techniques [15]. These surface-localized vibrational features were found to be weakened upon annealing to 110–150 K or exposure to acetylene or hydrogen sulphide [16], which reflects the disordered nature of the surface and near-surface regions. The reconstruction of the near-surface region of crystalline ice from the bulk-truncated arrangement that involves dangling H and O atoms on the ice surface is driven by the reduction of the amount of unsaturated surface groups through rearrangement toward a more disordered configuration. However, the near-crystalline arrangement of the near-surface region could be restored by hydrogen bonding between appropriate adsorbates and the topmost dangling H and O

groups of the reconstructed ice surface. Unlike the other surface modes, the vibrational modes of the OH db's are localized on individual surface complexes and can therefore be used as a sensitive probe for the nature of the surface (and near-surface) micro-structures of ice and the adsorbate-induced effects.

The surface area of ice micro-phases may vary greatly from 240–500 m^2/g for vapour-deposited low-density amorphous ice (due to the abundance of nano-scale pores in highly open network) [17] to 5–12 m^2/g corresponding to film structures without pores [18]. By comparing the amounts of surface areas of nc-ice and pc-ice deposited at 22–145 K by effusive beam dosing at different incident angles and by ambient dosing, Stevenson et al. showed that the surface area of the nc-ice deposits increases with a larger incident angle (from the normal direction) in qualitative accord with the predictions of the ballistic deposition model [19]. This model takes into general account of the interplay between roughening caused by randomness of deposition, smoothing by surface diffusion, and non-local effects generated by shadowing [20]. The unusually large values of surface area obtained by ambient dosing at 22 K (2700 m^2/g) and 77 K (640 m^2/g) along with the linear increase of the surface area with deposition time led Stevenson et al. to propose that the internal surface is directly connected to the external surface of the film. This observation is consistent with the grass-like or dendrite-like model for the morphology of the ice film. Furthermore, the adsorbate uptake by the ice films deposited by beam dosing at different incident angles above 90 K was found to be the same as that by the pc-ice films deposited at 145 K [19], which can be explained by enhanced surface diffusion at a higher temperature. With increasing deposition temperature, the surface area of the ice film was also found to be greatly reduced [19], suggesting isolation of the internal surface from the impinging gas molecules while the areas of the external surfaces of nc-ice and pc-ice films remain the same.

Previous studies by FTIR reflection–absorption (RA) spectroscopy have revealed the presence of OH db's on both the external and internal surfaces of vapour-deposited ice films, and further showed that the formation of the internal surface depends on the temperature and vapour pressure of the deposition [21–23]. In particular, a fast deposition rate at a lower temperature (e.g., below 130 K) favours the production of a porous amorphous water network with relatively well-developed internal surfaces. Under these growth conditions, the RA spectral signal of the OH db's comes primarily from the unsaturated OH groups located on the surface of micro-pores [23]. On the other hand, a higher deposition temperature favours the formation of denser structures with lower porosity and smoother surface, which is in good accord with the results reported by Stevenson et al. [19]. The presence of the OH db's on the external surface of cubic nano-crystals condensed at 83 K was observed by Delzeit et al. up to a post-annealing temperature of 145 K [16], which illustrates the substantive thermal stability of the surface structural elements containing these dangling bond groups. However, the OH db signal has been found to disappear in the case of thin amorphous ice films vapour deposited at 80 K upon post-annealing to the crystallization temperature ($\sim$155 K) [9,24]. It would therefore be of great interest to investigate the behaviour of OH db's in the ice micro-phases at temperatures above 150 K, where phase transition from amorphous ice to polycrystalline polymorphs begins.

2. FTIR reflection–absorption data of polycrystalline and non-crystalline ice films

In order to investigate the surface chemistry of ice micro-phases and their interactions with organic adsorbates, we have recently recorded the FTIR-RA spectra of ice films grown by vapour deposition at 128–185 K and characterized their nature as pc-ice or nc-ice phase by Fresnel reflection and Mie scattering calculations [25]. We show that pc-ice and nc-ice can be formed by vapour deposition above 155 K and below 145 K, respectively. For the early stage of film deposition of pc-ice and, to a certain extent, nc-ice, the good agreement between our experiment and the Mie scattering calculations generally confirms the heterogeneous character of the early deposits that

consist largely of small water aggregates. Upon further film growth, the experimental spectra are found to be in accord with the Fresnel model, illustrating the evolution to more homogeneous films.

Fig. 1 shows typical FTIR-RA spectra for the thicker ice films obtained at 83° incidence in a specular RA geometry in a home-built ultrahigh vacuum apparatus described in detail elsewhere [25]. The experimental spectra are compared with simulated spectra using the Fresnel equations for reflection coefficients (Fresnel spectra) for pc-ice and nc-ice of selected film thickness and appropriate optical constants for pc-ice [26] and nc-ice [27]. Evidently, there are two general types of spectral features: the characteristic vibrational modes of the ice films (stationary in positions) and the destructive interference patterns of the σ- and π-polarized components of the IR light that travel across the spectral region as a function of film thickness. Details of the spectral assignments have been given in our earlier work [25]. Briefly, three "stationary" vibrational modes of the ice phases are observed at 3600–2900 cm^{-1} (O–H stretching mode), 2245–2230 cm^{-1} (combination band) and 1650–1620 cm^{-1} (bending mode and/or the first overtone of hindered rotation). The good agreement between the experiment and the Fresnel spectra indicates that the evolution of the O–H stretch with film thickness can be attributed predominantly to the physics of RA of the IR light [28] and not to any possible changes in the water network structure during the film growth. The O–H stretching and bending modes of the nc-ice observed in the present work are blue-shifted while the combination band is slightly red-shifted with increasing film thickness in comparison with the respective vibrational bands for pc-ice, which is in good accord with data reported by Hardin and Harvey [6] and Hagen et al. [7]. In addition, σ-polarized interference patterns are found to shift from 3060 to 2520 cm^{-1} for pc-ice films (Fig. 1a), and from 3090 to 2520 cm^{-1} for nc-ice films (Fig. 1b) as the film thickness is increased from 550 to 1000 nm. The optical feature at 3780 cm^{-1} in Fig. 1a or at 3730 cm^{-1} in Fig. 1b corresponds to the emergence of another σ-polarized pattern. Similarly, spectral features corresponding to the π-polarized destructive interference pattern are found to travel from 3120 to 3075 cm^{-1} for pc-ice (Fig. 1a) and from 3145 to 3105 cm^{-1} for nc-ice (Fig. 1b) with increasing film thickness. Movements of these interference peaks could significantly distort the intensities and shapes of specific bands in a RA spectrum with increasing film thickness (e.g., the interference feature at 2520 cm^{-1} for 1000-nm-thick films), which in turn complicates spectral identification and population analysis of the corresponding groups in the case of solids.

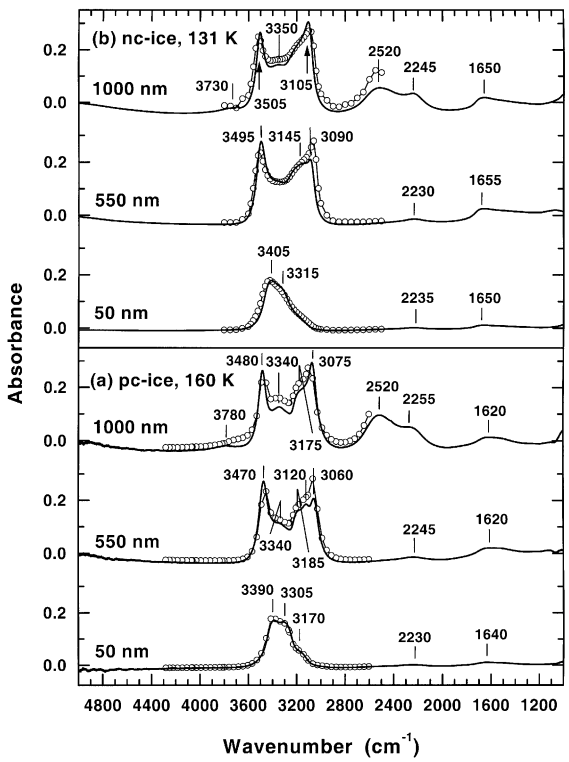

Fig. 1. Experimental RA spectra (solid lines) and simulated spectra (open circle lines) for (a) pc-ice and (b) nc-ice films of different thickness deposited at 1×10^{-6} Torr and 160 and 131 K, respectively. Simulated spectra are obtained by Fresnel equations for reflection coefficients using the appropriate optical constants for pc-ice and nc-ice obtained from the literature [26,27]. The indicated film thickness is obtained from optical interference measurement and found to be in good agreement with the thickness parameter used in the Fresnel simulation that gives the closest agreement with the respective experimental spectrum.

The change in the relative intensity of the weak OH db feature observed at 3700–3690 cm^{-1} [10] as

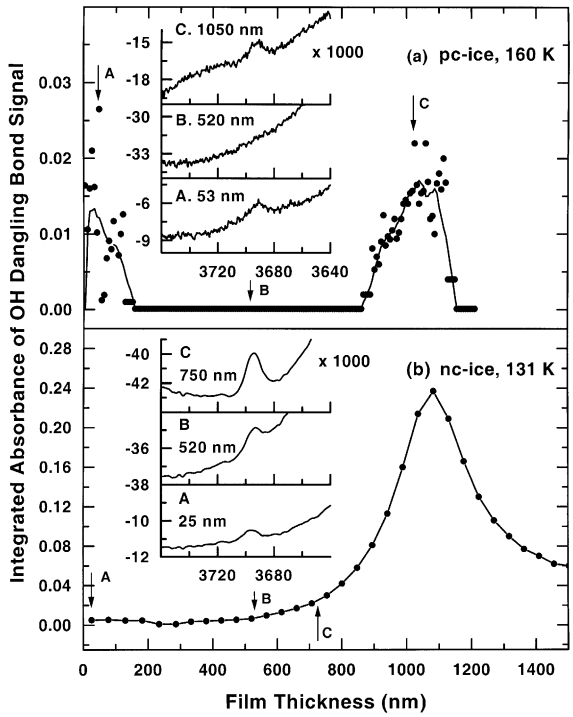

Fig. 2. Integrated absorbance of the OH db signal as a function of the film thickness for (a) pc-ice deposited at 160 K and 1×10^{-6} Torr, and (b) nc-ice deposited at 131 K and 5×10^{-6} Torr. The curves are used to guide the eyes only. The film thickness is estimated by optical interference method and found to be in reasonable agreement with the thickness parameter used in the respective Fresnel simulation. Inserts (with the ordinate expanded by 1000) show the OH db feature at selected film thicknesses marked by arrows.

a function of film thickness for pc-ice and nc-ice is shown in Fig. 2. According to the metal surface selection rule, only the OH db in the case of a thin ice film (below 100 nm) with a dipole moment component perpendicular to the metal surface could contribute to the RA signal. Any OH db with a dipole moment oriented parallel to the metal surface (e.g. that on the prism surfaces $(10\bar{1}0)$ of single-crystal hexagonal ice) could remain invisible to the IR-RA technique. Because of the randomized nature of the film growth process on non-single-crystal surfaces, the amount of OH groups with non-zero perpendicular dipole moment components is not known a priori. Despite the weak OH db feature relative to the O–H stretch feature, making it susceptible to spectral noise and baseline instability, the general trend in the behaviour of the OH db signal can be inferred and used to provide a more complete picture of the OH db formation in the surface chemistry of ice.

For films thinner than 120 nm, the OH db signals for both pc-ice and nc-ice are found to be weak and almost independent of the film thickness (Fig. 2). The spectral intensity of the OH db appears to diminish for pc-ice film 150–850 nm thick (deposited at 160 K) and recover to essentially the same level for films thicker than 850 nm. For nc-ice deposited at 131 K, on the other hand, the intensity remains relatively constant up to a film thickness of 600 nm and increases by over 20-fold in the 600–1400 nm thickness region. The emergence of the σ-polarized interference pattern in the optical window 3710–3680 cm^{-1} appears to significantly enhance the OH db signal for thick films [25]. This optical amplification in the signal intensity does not therefore necessarily correlate with the increase in the concentration of the OH db groups in the material. The same phenomenon has also been observed for other absorption bands in ice. Apparently, the amplification is much stronger in the case of nc-ice than pc-ice. In the latter case, essentially the same magnitude of the db signal for the 850–1150-nm-thick film relative to the thin film <120 nm) suggests that the lack of OH db signal in the intervening thickness region does not necessarily indicate the absence of OH db's, but rather it could be due to spectral interference of the O–H stretch that overwhelms the dangling bond feature (Fig. 2a). This observation indicates that the concentration of the OH db's on pc-ice could remain essentially the same with the film growth. Unlike the earlier reports, we observe the presence of OH db signal on pc-ice films deposited at temperature as high as 185 K. In addition, slow annealing of a 100-nm-thick pc-ice film (deposited at 160 K) to 185 K does not change the OH db signal despite the significant loss of ice (30%) to sublimation, which suggests that the OH db's are continuously being replenished in the sublimation process. The surface complexes containing the OH db's therefore appear to be stable over a wide temperature range of 128–185 K. These observations, together with the results reported by the earlier studies [10,21,22], lead us to

conclude that the OH db's are located on the external surface of the pc-ice films. In contrast to pc-ice films, the intensity of the db signal for nc-ice films thicker than 1400 nm is still significantly higher than that for thin films (<120 nm, Fig. 2b). This difference from pc-ice films suggests that the concentration of OH db's in nc-ice in fact increases with film growth, which is in general accord with the observation made by Zondlo et al. [23] that the concentration of OH db groups in low-density ice (obtained at ~94 K) increases with increasing film thickness. In order to account for the proportionality of the abundance of the OH db's with respect to the amount of ice, the latter work further concluded that the OH db's are located on the surfaces of multiple micro-pores inside the amorphous solid ice network [23]. The existence of the OH db's on the surfaces of open and close micropores has also been predicted for film growth of low-density ice under appropriate conditions by Zhdanov and Norton using Monte Carlo simulation [29]. For thin (~100 nm) nc-ice films, the OH db signal is found to persist upon annealing from 131 to 165 K, i.e., above the temperature of crystallization to cubic ice. The crystallization process appears not to affect the amount of OH db's significantly, with the surface structural elements containing the OH db's found to be stable towards thermal annealing and the extent of post-deposition. These results suggest that the OH db groups are located on the external surfaces of nc-ice films less than 100 nm thick (deposited above 130 K), which is in accord with the results by Stevenson et al. [19], Callen et al. [21] and Horn et al. [22]. For thicker films, the OH db's are thought to be on the external tracery surface of the deposits. The increase in the OH db signal (with origin from the surface) therefore indicates that the extent of the surface region also increases with increasing film thickness in the case of nc-ice.

3. Interactions of acetone with OH dangling bonds on ice films

In order to examine the role of the OH db's in the surface chemistry of the ice micro-phases, the adsorption of acetone (CH_3COCH_3, a soft Lewis base) on pc-ice and nc-ice films is investigated by FTIR-RA spectroscopy. Based on temperature programmed desorption and FTIR-RA data of acetone adsorbed on thin nc-ice film (<20 nm thick) at 95 K, Schaff and Roberts proposed that the interaction between the adsorbate and the ice surface involves hydrogen bonding between the carbonyl group of acetone and the OH db in ice [24]. For the pc-ice prepared by crystallization of the nc-ice post-annealed at 160 K, no OH db was observed and consequently neither was acetone–H–O db complex detected by Schaff and Roberts [24]. However, in the present work we observe the OH db signals for both pc-ice and nc-ice (Fig. 2). We therefore expect the formation of the acetone–H–O db complex involving hydrogen bonding to take place on these ice films. Fig. 3 shows the RA difference spectra for various exposures of acetone under different exposure pressure conditions on a 30-nm-thick pc-ice film (obtained by vapour deposition at 160 K followed by soaking at the base pressure for 30 min). The difference spectra correspond to the difference of RA spectra for ice films with and without the acetone exposures and therefore should reveal spectral features corresponding primarily to the acetone–ice complexes. The substrate spectrum of this pc-ice film of the aforementioned thickness has been shown to be best approximated by a model in between the Fresnel and Mie simulations, involving polycrystalline deposits with crystalline light-scattering particles and other film-like fragments [25].

For the exposure pressure of 1×10^{-7} Torr, the adsorption of acetone is manifested in the difference spectra (Fig. 3) by negative RA difference features in the OH db and the O–H stretching and bending regions, and by the positive RA difference features that correspond to the fundamentals of acetone, including the carbonyl stretch ($\nu_3(A_1)$) at 1701 cm^{-1}, asymmetric ($\nu_{21}(B_2)$), $\nu_4(A_1)$ and symmetric ($\nu_{16}(B_1)$, $\nu_5(A_1)$) CH_3 deformation bands at 1444, 1428, 1372 and 1362 cm^{-1} respectively, and asymmetric C–C stretch ($\nu_{17}(B_1)$) at 1242 cm^{-1}. The intensity of the carbonyl stretching band is found to saturate along with the negative OH db signal with increasing exposure (time), which provides strong evidence for the formation of a surface complex between acetone and

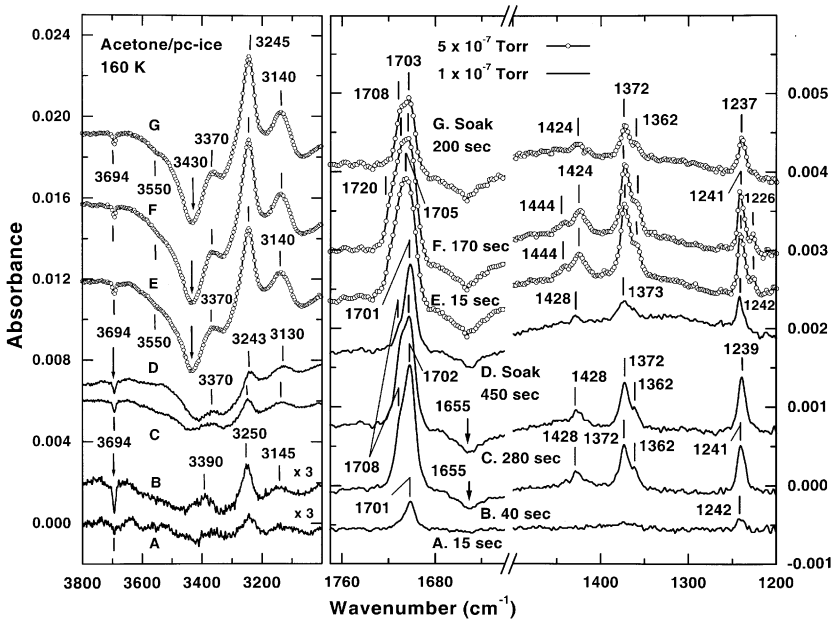

Fig. 3. Experimental RA difference spectra of acetone obtained under different conditions on a pc-ice film (~5 nm thick) deposited at 160 K and 5×10^{-7} Torr. The acetone exposures are performed at 160 K and 1×10^{-7} Torr for (A) 15, (B) 40 and (C) 280 s, and at 5×10^{-7} Torr for (E) 15 and (F) 170 s. A post-exposure soaking period at the ambient chamber pressure of 6×10^{-9} Torr for (D) 450 and (G) 200 s is performed after the acetone deposition in (C) and (F), respectively.

the surface OH db. The relative positions of the fundamental frequencies of the acetone–ice complex also support the hypothesis for the existence of hydrogen bonding in the adsorbate complex, given the red (blue) shift of the carbonyl stretch at 1701 cm^{-1} (asymmetric C–C stretch at 1242 cm^{-1}) found in the present case in comparison with that for pure liquid at 1710 cm^{-1} (1221 cm^{-1}) [30], isolated acetone matrix at 1725 cm^{-1} (1217 cm^{-1}) [30] and isolated acetone–water matrix at 1716 cm^{-1} (1230 cm^{-1}) [31]. These notable frequency shifts can therefore be attributed to the formation of strong hydrogen bonding between O of the carbonyl group in acetone and H of the OH db (referred as α-complex in the present work). However, the emergence of the high-frequency shoulder near 1708 cm^{-1} in the carbonyl stretch band (Fig. 3, Curve B) at a higher acetone exposure (time) indicates bounding of additional acetone molecules to surface water molecules and/or other acetone molecules possibly by electrostatic and van der Waals forces (β-complexes). The negative changes observed in the O–H stretching (3550 and 3430 cm^{-1}) and bending (1655 cm^{-1}) regions indicate the loss of ice signal due to acetone adsorption, which could be attributed to the ordering of the near-surface region (consistent with the picture proposed by Devlin and coworkers [14–16]) and to possible sublimation of the acetone–ice complexes. The group of positive peaks at 3370, 3243, and 3130 cm^{-1} can be attributed to the bulk modes of crystalline ice, the intensity of which are enhanced by adsorbate-induced ordering in the near-surface region of ice (Fig. 3, Curve C). The sublimation process of the acetone–water complexes exposes newly formed surface sites for further adsorption of incoming acetone molecules. The dynamic nature of the adsorption–desorption process is illustrated by the general reduction in the acetone fundamental features after the sample is left (soaking) at the ambient pressure of 6×10^{-9} Torr for a post-exposure period of 450 s (Fig. 3, Curve D). Furthermore, the reduction in intensity for the

high-frequency shoulder at 1708 cm^{-1} appears to be greater than that for the main carbonyl peak at 1701 cm^{-1}, suggesting a greater desorption rate for the β-complex (relative to the α-complex).

For acetone exposure at 5×10^{-7} Torr, the intensity of the carbonyl stretch saturates at a higher level (Fig. 3, Curve E) at 1.4 times of that for exposure at 1×10^{-7} Torr (Fig. 3, Curve B). For the acetone exposure pressure used in the present work, the coverage is found to be weakly dependent on the exposure pressure, which indicates possible transition from Langmuir-type adsorption driven by hydrogen bonding to more complex adsorption mechanisms that involve multilayer adsorption and acetone trapping into the ice. The presence of a new feature at 1226 cm^{-1} attributable to asymmetric C–C stretch and an additional broad shoulder at 1720 cm^{-1} in the carbonyl band, along with enhancement in intensity of the asymmetric deformational band at 1444 cm^{-1} (Fig. 3, Curves E and F), identify the emergence of a new acetone–ice complex (γ-complex in the present work). The structure of this γ-complex is thought to be similar to the acetone clathrate–hydrate due to similar adsorbate–water network interactions [32,33]. After the sample is allowed to soak at 160 K under an ambient pressure of 6×10^{-9} Torr for a post-exposure period of 200 s (Fig. 3, Curve G), the spectral features of the γ-complex are found to disappear, leaving only the β- and α-complexes on the surface. With the exception of the α-complex which involves strong hydrogen bonding between the carbonyl group and the OH db, the nature of the β- and γ-complexes remains ambiguous. The encapsulation of acetone molecules (γ-complex) in the surface structure of the pc-ice under certain acetone exposure conditions (above 160 K and 5×10^{-7} Torr) would further suggest the existence of disordered fragments in the near-surface structure of pc-ice, the rearrangement of which could in turn affect the dynamics of the formation of the acetone clathrate–hydrate intermediates [32].

Acetone adsorption experiments have also been performed on thin nc-ice films (with an estimated Fresnel thickness of 5 nm) deposited at 131 K (not shown). Despite the differences in the nature and film thickness of the ice film, similar behaviour in the adsorption of acetone (to that on pc-ice), with gradual saturation of the OH db signal along with a concomitant increase in the intensities of the acetone fundamentals, has been observed for acetone exposure pressure of 1×10^{-8} Torr. Furthermore, the saturation of the negative OH db signal for nc-ice at essentially the same level as that for pc-ice provides further evidence that the OH db's are located on the external surfaces of both thin pc-ice and nc-ice films. This result, together with the similarity in the FTIR-RA spectra for acetone adsorption on thin nc-ice and pc-ice films, suggests a similar surface structure for nc-ice and pc-ice in this thickness range (below 50 nm), consistent with the conclusions of Devlin and coworkers [14–16]. No spectral evidence has thus been found for the existence of OH db's in micropores or on other forms of internal surfaces in thin pc-ice and nc-ice films at 128–185 K, in accord with the results by Brown et al. [11], Stevenson et al. [19] and Zondlo et al. [23]. Furthermore, the adsorption of acetone appears to promote surface crystallization in the nc-ice film, which in some cases could lead to considerable reconstruction of the film structure.

In the case of pc-ice film 1100 nm thick deposited at 185 K, similar adsorption behaviour of acetone is also observed, with the intensity of the negative OH db signal after saturation by acetone found to be similar to those observed in the aforementioned cases. This result again supports the conclusion that OH db's are located on the external surface of thick pc-ice films, consistent with the dependence of the OH db signal on film thickness shown in Fig. 2.

To investigate the kinetic behaviour of acetone adsorption on pc-ice and nc-ice films 1200-nm thick (grown at 160 and 131 K, respectively), we expose acetone at 1×10^{-6} Torr on pc-ice and at 1×10^{-7} Torr on nc-ice at the respective substrate temperatures. Fig. 4 shows the integrated absorbance of the OH db feature (at 3694 cm^{-1}) and the carbonyl stretch (at ~1705 cm^{-1}) in the difference spectrum as a function of the acetone dosage (in units of 1×10^{-6} Torr s or Langmuir). It should be noted that the exposure pressure of acetone could significantly affect the composition of the acetone–ice complexes and the overall adsorbate coverage of the ice films, as illustrated in Fig. 3. The nc-ice

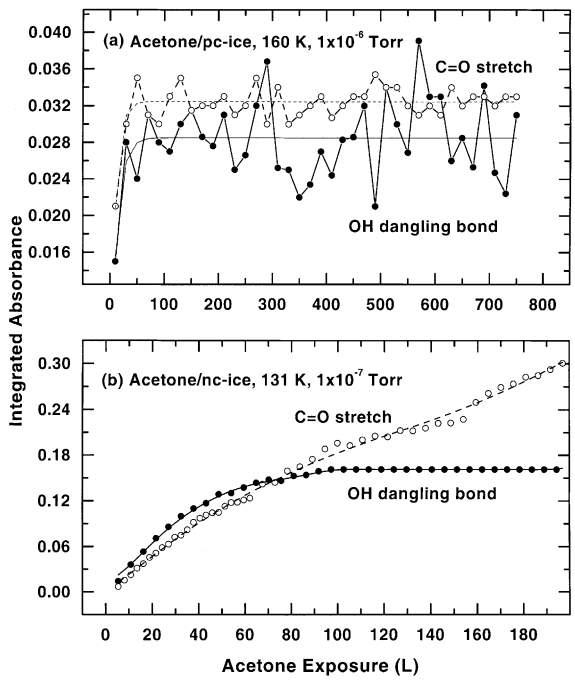

Fig. 4. Integrated absorbance of OH db (solid circle) and C=O stretch (open circle) features in the RA difference spectra as a function of acetone exposure at (a) 160 K and 1×10^{-6} Torr on a pc-ice film 1200 nm thick, and (b) 131 K and 5×10^{-7} Torr on a nc-ice film 1200 nm thick. The curves are used to guide the eyes only.

sample used in this experiment (Fig. 4b) exhibits a similar OH db intensity profile as a function of film thickness as that shown in Fig. 2b. Moreover, Fig. 2b shows the OH db intensity to be ~0.15 integrated absorbance unit for a film thickness of 1200 nm, which corresponds approximately to the same value as the loss of the db feature in the difference spectra at saturation (Fig. 4b). Fig. 4 shows that the amount of acetone adsorbed on both nc-ice and pc-ice films as approximated by the intensity of the respective carbonyl stretch bands is proportional to the amount of OH db's present in the ice structure. This proportionality is present as long as there is no formation of solid acetone phase, which might be difficult to avoid for acetone exposure at the lower temperature range (e.g., the deposition temperature of nc-ice near 131 K). Indeed, the continual growth of the carbonyl stretch band intensity for acetone adsorption on nc-ice (Fig. 4b) after OH db band saturation might be caused by physisorption of acetone. However, the markedly more intense RA signals observed for acetone adsorption on the nc-ice sample in comparison with the pc-ice case for the same exposure (e.g. at 100×10^{-6} Torr s) indicates that nc-ice has a significantly larger surface area than pc-ice, in general agreement with the results by Stevenson et al. [19] and Zondlo et al. [23]. The OH db's are located most likely on the external surface of nc-ice, which has a considerably higher convoluted tracery structure than pc-ice. The general increase in the intensity of the OH db's from 700 to 1400 nm observed for nc-ice (Fig. 2b) shows the evolution of the surface structure of nc-ice towards a more three-dimensional openwork structure that is accessible to gas exposure at the same time.

4. Concluding remarks

In summary, the OH db's (with characteristic features at 3700–3690 cm^{-1}) are an integral part of the nc-ice and pc-ice phases and they play a pivotal role in the surface chemistry of ice films. The surface structural elements containing these OH db's are found to be stable over a wide temperature range of 128–185 K covered in the present work. Unlike the earlier work, we also observe the OH db signal originated on pc-ice films deposited at temperature as high as 185 K. The thin nc-ice and pc-ice films contain comparable amounts of OH db's, which are located on the external surfaces of both phases with similar structures. The nature of the external surface (containing the OH db's) remains unchanged upon film growth for pc-ice with a general increase in the amount of OH db's, in contrast to film growth for nc-ice where the surface evolves into a more convoluted openwork structure. The acetone adsorption experiment shows that the acetone–H–O db complex is formed by hydrogen bonding between O of the carbonyl group in acetone and H of the H–O db in the ice film. In addition to the α-complex, more extensive structures (β- and γ-complexes) that involve interactions with other acetone molecules and substrate water molecules by electrostatic,

van der Waals and other mechanisms (including the intermediate formation of acetone clathrate–hydrate structures) can be observed at higher exposure pressure. The consequence of the presence of OH db's on the surface of pc-ice at relatively high temperatures may have significant implications on the types of plausible atmospheric surface reactions that could occur on and in ice in the important 190–220 K stratospheric temperature range.

Acknowledgements

This work is supported by the Natural Sciences and Engineering Research Council of Canada.

References

[1] A.L. Sumner, P.B. Shepson, Nature 398 (1999) 230.
[2] S. Solomon, R.R. Garcia, F.S. Rowland, D.J. Wuebbles, Nature 321 (1986) 755.
[3] M.J. Molina, L.T. Molina, C.E. Kolb, Ann. Rev. Phys. Chem. 47 (1996) 327.
[4] S.A. Sanford, Polarimetry of the interstellar medium, Astron. Soc. Pac. Conf. Series 97 (1996) 29.
[5] P.V. Hobbs, Ice Physics, Clarendon Press, Oxford, 1974, and references therein.
[6] A.H. Hardin, K.B. Harvey, Spectrochim. Acta. 29A (1973) 1139.
[7] W. Hagen, A.G.G.M. Tielens, J.M. Greenberg, Chem. Phys. 56 (1981) 367.
[8] P. Jenniskens, D.F. Blake, Science 265 (1994) 753.
[9] P. Jenniskens, S.F. Banham, D.F. Blake, M.R.S. McCoustra, J. Chem. Phys. 107 (1997) 1232.
[10] B. Rowland, M. Fisher, J.P. Devlin, J. Chem. Phys. 95 (1991) 1378.
[11] D.E. Brown, S.M. George, C. Huang, E.K.L. Wong, K.B. Rider, R.S. Smith, B.D. Kay, J. Phys. Chem. 100 (1996) 4988.
[12] G.P. Johari, Phil. Mag. B 78 (1998) 375.
[13] I. Kohl, E. Mayer, A. Hallbrucker, Phys. Chem. Chem. Phys. 2 (8) (2000) 1579.
[14] J.P. Devlin, V. Buch, J. Phys. Chem. 99 (1995) 16534.
[15] B. Rowland, N.S. Kadagathur, J.P. Devlin, V. Buch, T. Feldman, M.J. Wojcik, J. Chem. Phys. 102 (1995) 8328.
[16] L. Delzeit, M.S. Devlin, B. Rowland, J.P. Devlin, V. Buch, J. Phys. Chem. 100 (1996) 10076.
[17] J.A. Ghormley, J. Chem. Phys. 46 (1967) 1321.
[18] A.W. Adamson, L.M. Dormant, J. Am. Chem. Soc. 88 (1966) 2055.
[19] K.P. Stevenson, G.A. Kimmel, Z. Dohnálek, R.S. Smith, B.D. Kay, Science 283 (1999) 1505.
[20] A.-L. Barabási, H.E. Stanley, Fractal Concepts in Surface Growth, Cambridge, Cambridge University Press, 1995.
[21] B.W. Callen, K. Griffiths, P.R. Norton, Surf. Sci. Lett. 261 (1992) L44.
[22] A.B. Horn, M.A. Chesters, M.R.S. McCoustra, J.R. Sodeau, J. Chem. Soc. Faraday Trans. 88 (1992) 1077.
[23] M.A. Zondlo, T.B. Onasch, M.S. Warshawsky, M.A. Tolbert, G. Mallick, P. Arentz, M.S. Robinson, J. Phys. Chem. B 101 (1997) 10887.
[24] J.E. Schaff, J.T. Roberts, J. Phys. Chem. 98 (1994) 6900.
[25] S. Mitlin, K.T. Leung, J. Phys. Chem. (2002), in press.
[26] O.B. Toon, M.A. Tolbert, B.G. Koehler, A.M. Middelebrook, J. Geophys. Res. 99 (1994) 631.
[27] A. Leger, S. Gauthier, D. Deforneau, D. Rouan, Astron. Astrophys. 117 (1983) 164.
[28] M. Born, E. Wolf, Principles of Optics, sixth ed., Pergamon Press, New York, 1980.
[29] V.P. Zhdanov, P.R. Norton, Surf. Sci. 449 (2000) L228.
[30] G. Dellepiane, J. Overend, J. Spectrochim. Acta. 22 (1966) 593.
[31] X.K. Zhang, E.G. Lewars, R.E. March, J.M. Parnis, J. Phys. Chem. 97 (1993) 4320.
[32] D. Blake, L. Allamandola, S. Sanford, D. Hudgins, F. Freund, Science 254 (1991) 548.
[33] K. Consani, J. Phys. Chem. 91 (1987) 5586.